Characterization of Dominant Mechanisms in Contact Interface Restoring Forces

H. Jalali[11], H. Ahmadian[2]

[1]Department of Mechanical Engineering, Arak University of Technology, Arak 38135-1177, Iran.

[2]Centre of Excellence in Experimental Solid Mechanics and Dynamics, School of Mechanical Engineering, Iran University of Science and Technology, Tehran, Iran

Abstract

Accurate representation of different parts of a mechanical system is important in construction of mathematical models for structural dynamic analysis. There are usually elements in structures- for example joints or boundary conditions- which demand more efforts for precise modeling. This is due to development of the contact mechanisms- i.e. linear or nonlinear- in normal and tangential directions of their surfaces. In this paper a method for multiple nonlinearity detection and identification is proposed. The method is applied to characterize the state of the contact mechanisms in normal and tangential directions of a nonlinear beam subjected to a frictional contact support.

Keywords: contact interface, nonlinearity, parameter identification

1. Introduction

In modeling mechanical structures there are usually elements such as joints or boundary conditions which demand more efforts for precise representation. In fact the behavior of these elements depends upon the amplitude of the external forces applied to the structure. Usually their behavior is linear under

[1] *Corresponding author, email address: jalali@iust.ac.ir, tel.: +98 861 3670024, fax.: +98 861 3670020.*

low level excitation forces and under high level excitation forces nonlinearity arises leading to nonlinear dynamic response of the structure. The other feature of these elements is that the nonlinear mechanisms can develop both in normal and tangential directions of their contact interface. Therefore, in modeling stage, one faces a problem with multiple unknown elements which needs to be characterized.

The first step in modeling these elements is to decide if under certain excitation amplitude a linear or nonlinear model should be used. This can be done by employing nonlinearity detection methods. A comprehensive literature survey in this regard is done in the remaining of this section. The aim of this paper is to represent a method which can be used for multiple nonlinearity detection and parameter identification in structural dynamics.

Nonlinearity detection has been considered by many researchers in the past. Nonlinearity detection by using Hilbert transform is described in [1]. In [2] the complex stiffness method is used for detection and identification of the nonlinearity in SDOF systems. [3] and [4] uses the concept of nonlinear normal modes for nonlinearity detection and characterization. The reciprocal modal vectors have been suggested in [5]. The backbone (skeleton) curve [6] and more recently principal component analysis (PCA) [7] are also used for nonlinear behavior detection. The describing functions method has been used for nonlinearity detection and identification in [8, 9].

In this paper a multiple nonlinearity detection method is proposed. The method uses a number of measured frequency response functions (FRFs) of the nonlinear system and the FRF matrix of a reference linear system and identifies the state of the behavior of the unknown elements, i.e linear or nonlinear, by applying Sherman-Morison formula. The number of measured FRFs must be at least equal to the unknown elements. The advantage of this method is that the FRF measurement at the location of unknown elements is not needed. The accuracy of the proposed method is validated by using simulated data from a 2DOF nonlinear system and experimental data from a clamped beam subjected to a frictional boundary condition. The contact mechanisms in normal and tangential directions of the frictional interface are characterized. Next section considers description of the proposed method.

2. The proposed method

Consider a MDOF vibratory system consisting of *r* grounded unknown elements as is shown in Fig. (1-a). The behavior of these unknown elements may be linear or nonlinear. In this paper a method is proposed for detecting the state of the behavior of the unknown elements, i.e. linear or nonlinear. Since the proposed method is based on the frequency response functions (FRFs), it is convenient to approximate the nonlinear system with an equivalent linear system. Therefore under harmonic excitation condition the equivalent linear system presented in Fig. (1-b) can be replaced with the nonlinear system at each excitation frequency [8, 9]. By using the equivalent linear system, the FRFs of the nonlinear system can be obtained as is described in the remaining of this section. The aim of this paper is to propose a method which can be used for obtaining the equivalent linear stiffness coefficients k_i, *i=1,2,…,r,* by using the measured responses of the nonlinear system. The method is described in the following.

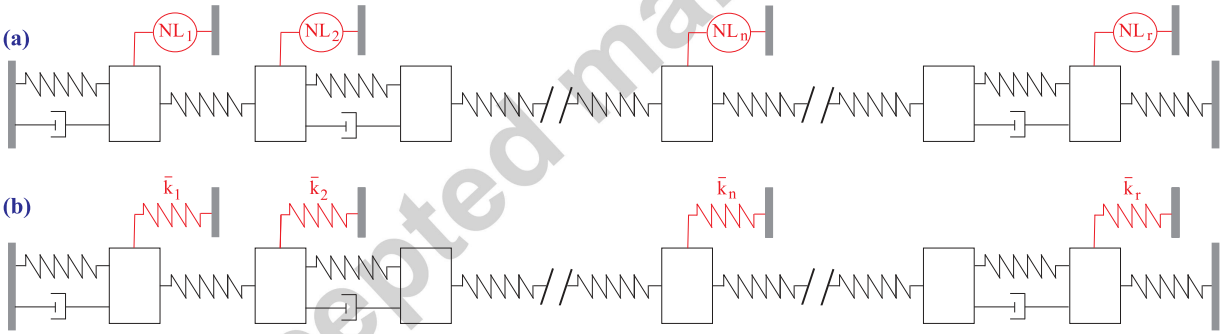

Figure 1- the nonlinear MDOF system (a) and its equivalent linear representative

The equation governing the motion of the system shown in Fig. (1-a) can be expressed in the matrix form as,

$$[\mathbf{M}]\{\ddot{x}\}+[\mathbf{C}]\{\dot{x}\}+[\mathbf{K}]\{x\}+\{N(x,\dot{x})\}=\{f\} \qquad (1)$$

where **M**, **C** and **K** are respectively mass, viscous damping and stiffness matrix of the system. *{f}* and *{N}* respectively represent the external forcing vector and the vector of internal nonlinear forces containing

the restoring force equation of the nonlinear elements. By considering harmonic excitation and assuming harmonic response at the same frequency, i.e.

$$\{f\} = \{F\} e^{j\omega t}, \qquad \{x\} = \{X\} e^{j\omega t} \tag{2-3}$$

one may cast the vector of the nonlinear forces *{N}* in the matrix form as [10, 11],

$$\{N(x, \dot{x})\} = [\boldsymbol{\Delta}(X, \omega)]\{X\} e^{j\omega t} \tag{4}$$

In Eq. (4) $\boldsymbol{\Delta}$ is a matrix containing the describing function representation of the unknown elements. $\boldsymbol{\Delta}$ can be expressed according to Fig. (1-b) as,

$$[\Delta] = \sum_{i=1}^{r} [\overline{\mathbf{K}}_i] \tag{5}$$

where $\overline{\mathbf{K}}_i$, $i = 1,2,...,r$ is a unit rank matrix and the elements of its α_i row can be defined as,

$$[\overline{\mathbf{K}}_i]_{\alpha_i,\beta} = \bar{k}_i(X_{\alpha_i}, \omega)\delta_{\alpha_i\beta} \tag{6}$$

where δ is the kronecker delta. It should be noted that i^{th} unknown grounded element is attached to α_i DOF. Therefore the equivalent linear stiffness $\bar{k}_i$ is a function of the response amplitude of α_i DOF, i.e. X_{α_i}, at excitation frequency ω.

By substituting equations (2-4) into equation (1) the FRF matrix of the system shown in Fig. (1-a) can be derived as,

$$[\overline{\mathbf{H}}(X, \omega)] = [\overline{\mathbf{Z}}(\omega)]^{-1} = \left([\mathbf{Z}(\omega)] + [\boldsymbol{\Delta}(X, \omega)]\right)^{-1}. \tag{7}$$

where, $\mathbf{Z}(\omega)$ is the dynamic stiffness matrix of the reference linear system,

$$[\mathbf{Z}(\omega)] = [\mathbf{H}(\omega)]^{-1} = [\mathbf{K}] - \omega^2[\mathbf{M}] + j\omega[\mathbf{C}]. \tag{8}$$

Equation (7) relates the FRF matrix of the nonlinear system to the FRF matrix of the reference linear system. In order to find the relationship between a measured nonlinear FRF, i.e. $\bar{h}_{pq}$, the equivalent

linear stiffness coefficients $\bar{k}_i, \quad i = 1,2,...,r$ and the elements of the FRF matrix of the reference linear system the Sherman-Morisson formula [12] as is described in the following can be used.

First let consider that Δ is a unite rank matrix- being referred to in the following as Δ'- and the elements of its l^{th} row can be defined as,

$$[\Delta']_{l,\beta} = \Lambda \delta_{l\beta} \tag{9}$$

By using equation (7) and the Sherman-Morisson formula [12] one can obtain,

$$[\bar{\mathbf{H}}] = [\mathbf{H}] - \frac{1}{1+g}[\mathbf{H}][\Delta'][\mathbf{H}] \tag{10}$$

where $g = tr\,[\Delta'][\mathbf{H}]$.

After some algebraic manipulations and matrix operations and by using the advantage of Δ' being a unit-rank matrix, the following equation is obtained,

$$\bar{h}_{pq} = h_{pq} - \Lambda \frac{h_{pl}h_{lq}}{1+\Lambda h_{ll}} \tag{11}$$

Equation (11) is used in the following to cast the relationship between a measured nonlinear FRF, the equivalent linear stiffness coefficients $\bar{k}_i, \quad i = 1,2,...,r$ and the elements of the FRF matrix of the reference linear system.

In order to use equation (11), first equation (7) is re-written in the following form,

$$[\bar{\mathbf{H}}(X,\omega)] = \left([\mathbf{Z}_1(\omega)] + [\bar{\mathbf{K}}_r(X,\omega)]\right)^{-1} \tag{12}$$

where,

$$[\mathbf{Z}_1] = [\mathbf{Z}] + \sum_{i=1}^{r-1}[\mathbf{K}_i] \tag{13}$$

In equation (12) $\bar{\mathbf{K}}_r$ is a unit rank matrix (equation (6)). By using equations (11) and (12) one can obtain,

$$\bar{h}_{pq} = (h_{pq})_1 - \bar{k}_r \frac{(h_{p\alpha_r})_1 (h_{\alpha_r q})_1}{1 + \bar{k}_r (h_{\alpha_r \alpha_r})_1} \tag{14}$$

where $(h_{--})_1$ corresponds to $[\mathbf{H_1}] = [\mathbf{Z_1}]^{-1}$. From equation (13) we have,

$$[\mathbf{H_1}] = [\mathbf{Z_1}]^{-1} = \left([\mathbf{Z_2}] + [\mathbf{K_{r-1}}]\right)^{-1} \tag{15}$$

where $\overline{\mathbf{K}}_{\mathbf{r-1}}$ is a unite rank matrix according to equation (6) and,

$$[\mathbf{Z_2}] = [\mathbf{Z}] + \sum_{i=1}^{r-2} [\mathbf{K_i}] \tag{16}$$

By using equations (11) and (15) the following equation is obtained,

$$(h_{pq})_1 = (h_{pq})_2 - \bar{k}_{r-1} \frac{(h_{p\alpha_{r-1}})_2 (h_{\alpha_{r-1} q})_2}{1 + \bar{k}_{r-1} (h_{\alpha_{r-1}\alpha_{r-1}})_2} \tag{17}$$

$(h_{--})_2$ is obtained from $[\mathbf{H_2}] = [\mathbf{Z_2}]^{-1}$. It is worth mentioning that equation (17) makes it possible to calculate $(h_{p\alpha_r})_1$, $(h_{\alpha_r q})_1$ and $(h_{\alpha_r \alpha_r})_1$ to be substituted into equation (14). The same procedure as in equations (15-17) has to be followed for each equivalent linear stiffness. By repeating *n* times this procedure one may arrive to equation (18),

$$(h_{pq})_n = (h_{pq})_{n+1} - \bar{k}_{r-n} \frac{(h_{p\alpha_{r-n}})_{n+1} (h_{\alpha_{r-n} q})_{n+1}}{1 + \bar{k}_{r-n} (h_{\alpha_{r-n}\alpha_{r-n}})_{n+1}} \tag{18}$$

By using equation (18) finally we have,

$$(h_{pq})_{r-2} = (h_{pq})_{r-1} - \bar{k}_2 \frac{(h_{p\alpha_2})_{r-1} (h_{\alpha_2 q})_{r-1}}{1 + \bar{k}_2 (h_{\alpha_2 \alpha_2})_{r-1}} \tag{19}$$

$$(h_{pq})_{r-1} = h_{pq} - \bar{k}_1 \frac{h_{p\alpha_1} h_{\alpha_1 q}}{1 + \bar{k}_1 h_{\alpha_1 \alpha_1}} \tag{20}$$

In equation (20), h_{pq}, $h_{p\alpha_1}$, $h_{\alpha_1 q}$ and $h_{\alpha_1 \alpha_1}$ are obtained from the reference linear system. By back-substitution from equation (20) to equation (17) and then equation (14) one can arrives to a nonlinear equation of the following form,

$$\bar{h}_{pq}(\omega) - h_{pq}(\omega) = g\left(\{d\}, \{h(\omega)\}\right) \tag{21}$$

In equation (21) $\{d\} = [\bar{k}_1, \bar{k}_2, ..., \bar{k}_r]^T$ is the vector of the unknown equivalent stiffness coefficients, $\{h\} = [h_{11}, h_{12}, h_{13}, ...]^T$ is a vector composed of the elements of the FRF matrix of the reference linear system and *g* is a nonlinear function. It is worth mentioning that equation (21) is formed at each excitation frequency and contains *r* unknown elements. Therefore at least *r* measured FRFs of the nonlinear system is needed to calculate the unknowns by solving equation (21) numerically. The equivalent linear stiffness can be used to detect whether the behavior of the unknown elements is linear or nonlinear. In Next section the proposed method is verified by using a numerical example.

3. Numerical example

A 2DOF system as is shown in figure (2) is considered,

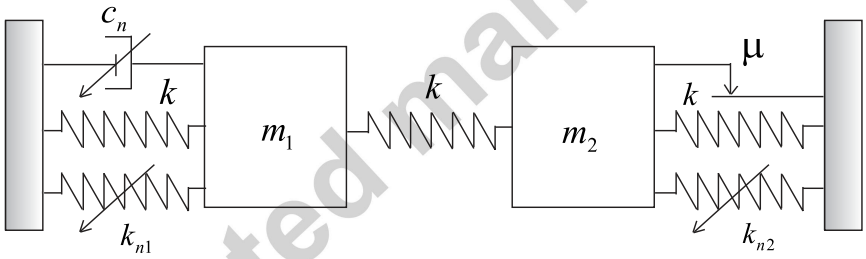

Figure 2- Two DOF system, $m_1 = 1$, $m_2 = 2$, $k = 100$

In equation (22) the governing equation of the dynamic response of the 2DOF system is presented. The system is considered to be excited using a harmonic force.

$$\begin{bmatrix} 1 & 0 \\ 0 & 2 \end{bmatrix} \begin{Bmatrix} \ddot{x}_1(t) \\ \ddot{x}_2(t) \end{Bmatrix} + \begin{bmatrix} 2 & -1 \\ -1 & 2 \end{bmatrix} \begin{Bmatrix} x_1(t) \\ x_2(t) \end{Bmatrix} + \begin{Bmatrix} N_1(t) \\ N_2(t) \end{Bmatrix} = 0.8 \begin{Bmatrix} 0 \\ sin(\omega t) \end{Bmatrix} \tag{22}$$

where,

$$N_1(t) = -k_{n1} x_1(t)^3 + c_n \,|\, \dot{x}_1(t) \,|\, \dot{x}_1(t), \qquad N_2(t) = -k_{n2} x_2(t)^3 + \mu \; sgn(\dot{x}_2(t)) \tag{23-24}$$

By solving equations (22) numerically for $k_{n1}=500$, $k_{n2}=750$, $c_n=1$ and $\mu=0.1$ at each excitation frequency ω the steady state response is obtained. Having the steady state response and the excitation force signals and transferring them into frequency domain by using the Fourier transform, the FRFs are obtained as,

$$\bar{h}_{pq}(\omega)=\frac{X_p(\omega)}{F_q(\omega)}e^{j\psi} \tag{25}$$

where X_p and F_q are respectively the amplitude of the steady state response and excitation force at frequency ω. ψ is the phase difference between excitation force and structural response signals. The frequency response functions as depicted in figure (3). In order to construct the equivalent stiffness coefficient for $N_1(t)$ and $N_2(t)$ the method described in previous section is employed.

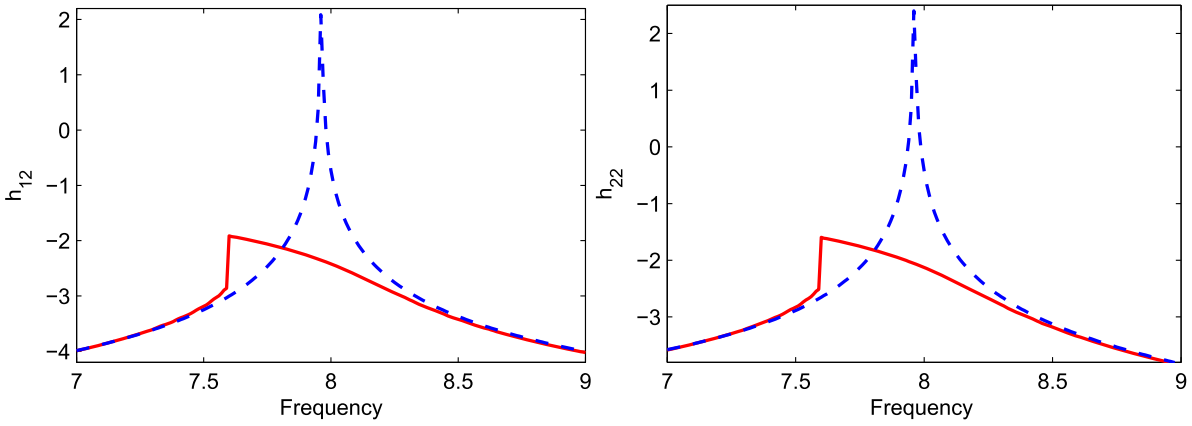

Figure 3- The FRFs of the nonlinear system (solid) and the reference linear system (dashed)

By following the procedure described in previous section one can obtain,

$$\bar{h}_{pq}=(h_{pq})_1-\bar{k}_2\frac{(h_{p2})_1(h_{2q})_1}{1+\bar{k}_2(h_{22})_1} \tag{26}$$

$$(h_{pq})_1=h_{pq}-\bar{k}_1\frac{h_{p1}h_{1q}}{1+\bar{k}_1h_{11}} \tag{27}$$

Computing $(h_{p2})_1$, $(h_{2q})_1$ and $(h_{22})_1$ by using equation (27) and substituting them along with $(h_{pq})_1$ into equation (26) the following equation is formed,

$$\bar{h}_{pq} - h_{pq} = -\bar{k}_1 \frac{h_{p1}h_{1q}}{1+\bar{k}_1 h_{11}} - \frac{\left[h_{p2}\left(1+\bar{k}_1 h_{11}\right) - \bar{k}_1 h_{p1}h_{12}\right]\left[h_{2q}\left(1+\bar{k}_1 h_{11}\right) - \bar{k}_1 h_{21}h_{1q}\right]}{\left(\frac{1}{\bar{k}_2} + h_{22}\right)\left(1+\bar{k}_1 h_{11}\right) - \bar{k}_1 h_{21}h_{12}} \tag{28}$$

Equation (28) relates the measured nonlinear FRF to the FRFs of the reference linear system and the equivalent linear stiffness coefficients $\bar{k}_1$ and $\bar{k}_2$. This is an equation with two unknowns, i.e. $\bar{k}_1$ and $\bar{k}_2$. Therefore having measured two nonlinear FRFs the unknowns can be identified at each excitation frequency. Since excitation is applied on m_2 therefore in equation (28) $q = 2$. By taking $p = 1$ and $p = 2$ and using the FRF matrix of reference linear system equation (28) results in two nonlinear equations. By solving these equations numerically $\bar{k}_1$ and $\bar{k}_2$ are obtained at each frequency. The nonlinear FRFs to be used in equation (28) are $\bar{h}_{12}$ and $\bar{h}_{22}$ which are shown in Figure (3). The FRF matrix of the reference linear system is obtained from,

$$[\mathbf{H}(\omega)] = \left([\mathbf{K}] - \omega^2[\mathbf{M}]\right)^{-1} \tag{29}$$

Figure (4) shows the calculated equivalent stiffness coefficients $\bar{k}_1$ and $\bar{k}_2$,

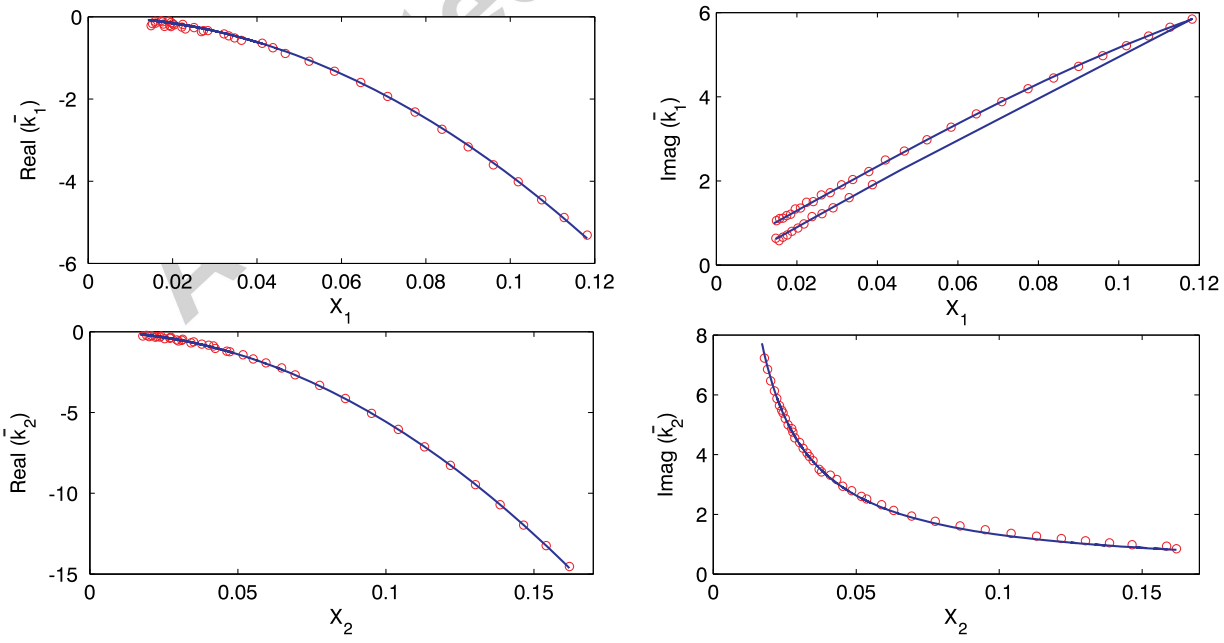

Figure 4- Equivalent stiffness coefficients, calculated (circles) and fitted (solid lines)

Since the imaginary and real parts of the equivalent linear stiffness coefficients shown in figure (4) changes with the amplitude of the system response, this indicates the presence of the nonlinearity in the system. By employing the describing functions concept [13] the equivalent linear stiffness of nonlinear elements described by equations (23) and (24) are obtained as,

$$\bar{k}_1 = -\frac{3}{4}k_{n1}X_1^{\,2} + j\frac{8}{3\pi}c_n X_1\omega^2, \qquad \bar{k}_2 = -\frac{3}{4}k_{n2}X_2^{\,2} + j\frac{4\mu}{\pi X_2} \tag{30-31}$$

where X_1 and X_2 are the response amplitude of m_1 and m_2 at excitation frequency ω. By fitting equations (30) and (31) on the results presented in figure (4) the nonlinear parameters, i.e. k_{n1}, k_{n2}, c_n and μ, can be identified. In Table (1) the exact and identified parameters are compared.

Table 1- Comparison of the exact and identified parameters

	k_{n1}	k_{n2}	c_n	μ
Exact	*500*	*750*	*1.0*	*0.1*
Identified	*514.667*	*743.113*	*1.009*	*0.103*
Error (%)	*2.9*	*-0.9*	*0.9*	*3.0*

The results presented in Table (1) as well as the results shown in figure (4) indicate the accuracy of the proposed method in this paper. The method is applied to experimental results in next section.

4. Experimental validation

Nonlinearity in a contact interface can arise both in normal and tangential directions depending on the amplitude of the excitation forces [14, 15]. Usually under low level excitation force amplitudes contact interfaces behave linearly. By increasing the excitation amplitude, nonlinear mechanisms develop causing nonlinearity in the dynamic response of the structure. Detecting whether the behavior of the contact interface is linear or nonlinear is helpful in proposing proper models for the dynamics of the contact interface. In this section nonlinearity detection and identification in normal and tangential directions of a frictionally supported beam is considered.

4.1. Test set-up

Figure (5) shows the experimental test rig which consists of a clamped beam. The other end of the beam is subjected to a frictional contact support (point O). A constant normal force

($\approx 150\ \ N$) provided by mass blocks is applied to the contact interface. The linear or nonlinear contact mechanisms may occur respectively in tangential and normal directions of the contact support if the amplitude of the excitation forces is sufficient to excite them. The aim of this section is to detect the state of the behavior of the mechanisms at the contact support- i.e. linear or nonlinear- and to identify there parameters by using the method described in previous section.

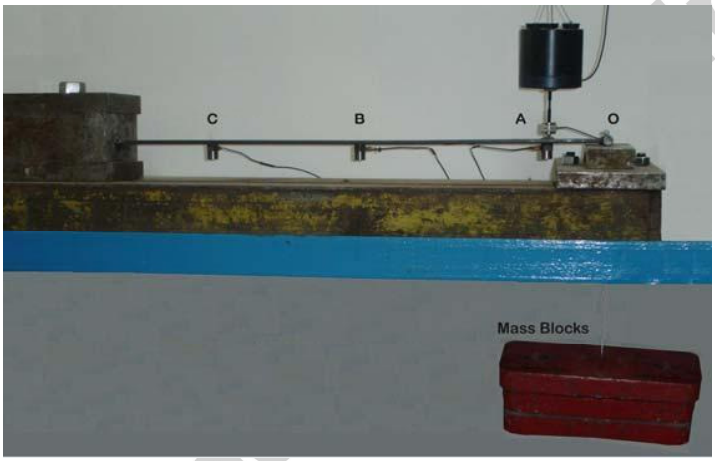

Figure 5- Experimental test set-up

The beam is excited by means of an electromagnetic shaker at point A and its response is measured at points A, B and C. First, low level random excitation is used and the FRFs are measured. The level of random excitation is tuned such that it makes sure that the response of the structure is linear. The linear FRFs are used later in this section and the reference linear system is constructed. Figure (6) shows two linear FRFs.

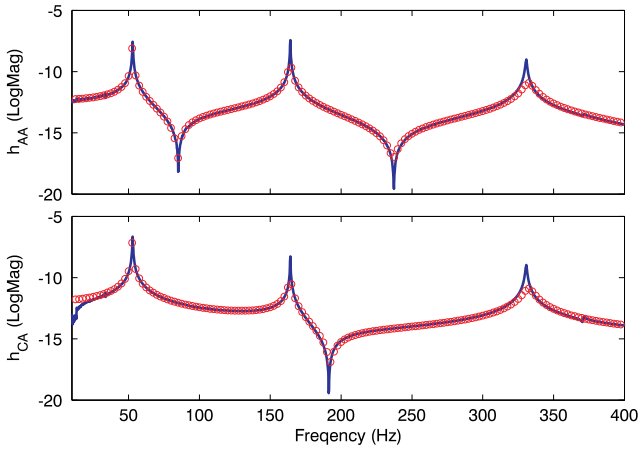

Figure 6-Comparison of the experimental FRFs (solid lines) and the FRFs obtained from reference linear system (circles)

Next, different sine sweep excitations at different amplitudes and with frequency ranges around the first natural frequency of the structure are applied to the structure. It is expected that by increasing the excitation amplitude level the nonlinear mechanisms develop at the contact interface. Figure (7) shows the measured FRFs by sine sweep excitation method,

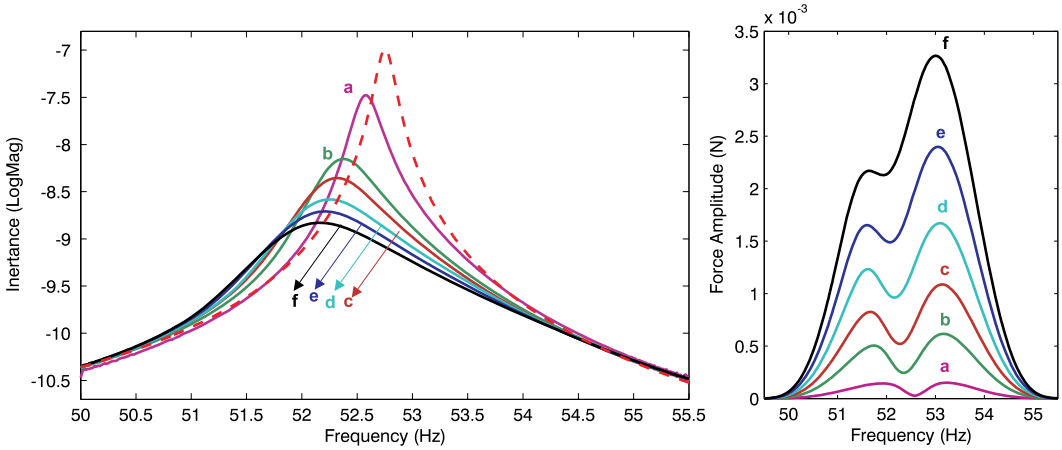

Figure 7- Left: Direct FRFs obtained by sine sweep (solid) and random (dashed) excitations, right: force amplitudes used in sine sweep excitation

The FRFs shown in Figure (7) indicate presence of nonlinearity in the system since there peak amplitude and frequency change as the excitation amplitude is increased. The decrease of the peak amplitudes and

resonant frequencies indicate respectively nonlinearity in stiffness and damping characteristics of the contact interface. It is not obvious from FRFs in figure (7) that at each excitation case which nonlinear mechanism- i.e. in normal or tangential direction- develops at the contact interface. Detection of the state of the contact mechanisms is done by using the method proposed in this paper as is described in the following.

4.2. Reference linear system

In order to employ the method described in previous sections, a reference linear system is needed. The reference linear system can be constructed by using the measured linear FRFs shown in Figure (6). A finite element (FE) model is constructed for the beam structure by using 2D Euler-Bernoulli beam elements. The effects of contact mechanisms in normal and tangential directions are considered in the FE model by lateral and torsional springs as is depicted in figure (8a).

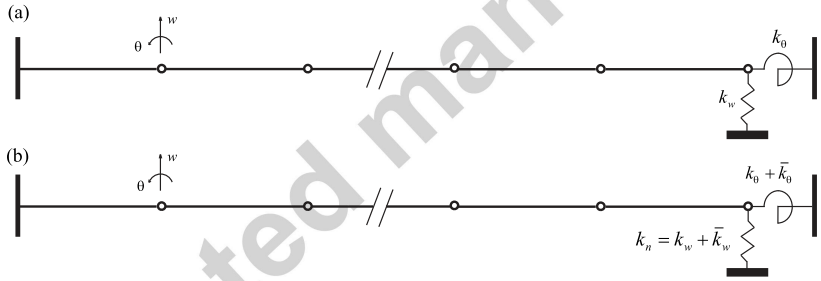

Figure 8- The reference linear system (a) and the equivalent linear system (b)

In normal and tangential directions the behavior of the contact interface may be linear or nonlinear. In normal direction two surfaces may be always in contact or experience separation. At low level excitation and when the contact point is compressed against the underlying steel block, elastic deformations occur in contact interface. At this condition the behavior of the contact interface in normal direction is linear. If the amplitude of the applied loads is increased, microscopic impacts develop between contacting surfaces and absorb a small amount of energy. The main feature of this micro-vibro-impact mechanism is dissipating energy in a nonlinear fashion. Therefore the micro-vibro-impact is characterized by linear stiffness but nonlinear damping mechanisms. When the amplitude of the applied loads is further increased such that the contacting surfaces completely separate from each other and come to contact repeatedly, the macro-vibro-impact happens. The main feature of macro-vibro-impact is transferring

energy to higher frequencies than those excite the impact mechanism [15]. Leaking energy to higher frequencies prevent defining a frequency response function. Therefore the method proposed in this paper which is based on frequency response functions can not be used to identify this mechanism. Time domain approaches, e.g. force-state mapping method, are more suitable for identification of macro-vibro-impacts [16].

When the contact point moves in opposite direction, the stiffness of the flexible wire used to suspend the mass blocks (see figure 5) plays the role of the stiffness in the normal direction. Therefore the stiffness of the contact point in normal direction is bilinear. A schematic of the normal contact force up to the macro-vibro-impact mechanism is depicted in figure (9a). A system with bilinear stiffness is inherently nonlinear; for the contact interface used in this paper the stiffness changes at zero penetration. Such a nonlinear system shows homogeneity in frequency domain [17]. Therefore the bilinear stiffness can be approximated by an equivalent linear stiffness for analysis in frequency domain. The linear behavior of the contact interface in normal direction is modeled by using a lateral spring of constant k_w in figure (8a).

In tangential direction the contact interface experiences three different regimes- stick, partial slip and gross slip- depending on the amplitude of the external force. At low amplitude forces the contact interface is in stick regime and behaves linearly. When the amplitude of the external force is increased, small regions in the contact interface start to slip (i.e. partial slip phase) leading to decreasing the stiffness of the contact interface in tangential direction. By further increasing the amplitude of the external force, bigger slip regions develop in the contact interface. Finally, the whole contact interface starts to slip and the gross slip occurs. The behavior of the contact interface in partial (or micro) and gross (or macro) slip is nonlinear. A schematic of the tangential contact force up to the macro-slip mechanism is depicted in figure (9b). The bending effect of the tangential contact force *R(t)* in stick phase is modeled as a torsional spring in the reference linear system shown in figure (8a). In the remaining of this paper the state of the contact interface mechanisms in normal and tangential directions is identified.

In figure (9c) a schematic of normal and tangential contact forces is shown. The surfaces are in contact when *N(t)* is less than the sum of *P* and the internal beam shear force and experience separation otherwise. *N(t)* is the normal contact force and *P* is the applied constant force. *A(t)*, *V(t)* and *M(t)* are respectively internal axial force, shear force and bending moment of the beam.

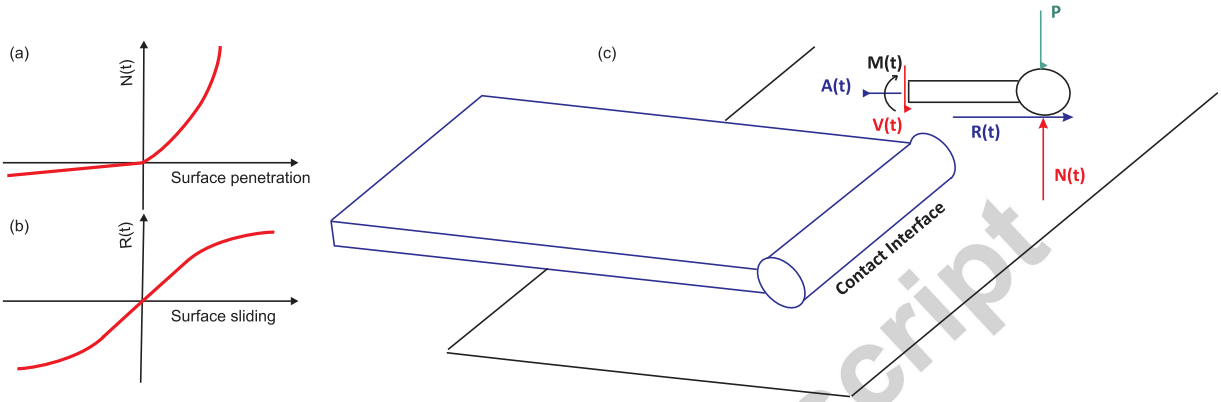

Figure 9- Schematic of the normal contact force (a) and tangential contact force (b); Normal and tangential contact forces acting at the contact interface (c).

In the FE model shown in Figure (8a), *L*=600 mm as length, *E*=211 GPa as module of elasticity, $\rho = 7860\ Kg/m^3$ as mass density and *b*=40 mm and *h*=5 mm as cross sectional dimensions of the beam are used. The stiffness coefficients of the lateral and torsional springs are identified such that the reference linear system generates the linear FRFs (Figure 6). Parameter identification is done by using eigen-frequency sensitivity method [18]. In the identification procedure three first natural frequencies are used. It is worth mentioning that a viscous damping matrix proportional to stiffness matrix is considered for the reference linear system, i.e. $[C] = 1\times10^{-5}[K]$. The identified values for lateral and torsional spring coefficients are $k_w = 1\times10^7\ N/m$ and $k_\theta = 152\ Nm/rad$.

Due to the location of the contact interface in the structure the natural frequencies are much more sensitive to the tangential contact stiffness k_θ than the normal contact stiffness k_w. For example the ratio of the sensitivity with respect to k_θ to the sensitivity with respect to k_w for the first natural frequency is 65. This ratio for the second and third natural frequencies is 70 and 1.7, respectively. This

means that mainly the third natural frequency controls k_w in the identification procedure. Therefore $k_w = 1\times10^7\ N/m$ is not the optimum value which controls the response of the structure around the first mode. This is an initial value which will be modified later in this paper when the response of the structure around the first mode and at different excitation amplitudes is considered.

The reference linear system is used in next section and the state of the contact mechanisms in normal and tangential directions are characterized.

4.3. Nonlinearity detection and identification

In order to detect the state of the contact mechanisms in normal and tangential directions, two complex springs, i.e. $\bar{k}_w$ and $\bar{k}_\theta$, are added to the reference linear system parallel to grounded springs k_w and k_θ (see figure 8b). $\bar{k}_w$ and $\bar{k}_\theta$ are considered as the equivalent linear models- or describing functions- for the contact mechanisms in normal and tangential directions, respectively. The values of $\bar{k}_w$ and $\bar{k}_\theta$ can be identified at different excitation amplitudes and frequencies by employing the method described in previous section and using the reference linear system shown in figure (8a). The real part of $\bar{k}_w$ is shown in Figure (10). Its imaginary part is found zero. The real and imaginary parts of the identified $\bar{k}_\theta$ are presented in figures (11) and (12).

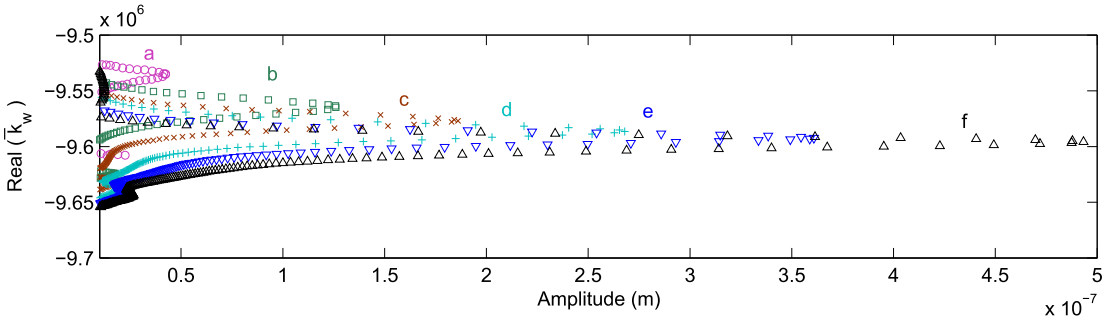

Figure 10- Real part of $\bar{k}_w$ at different excitation amplitudes

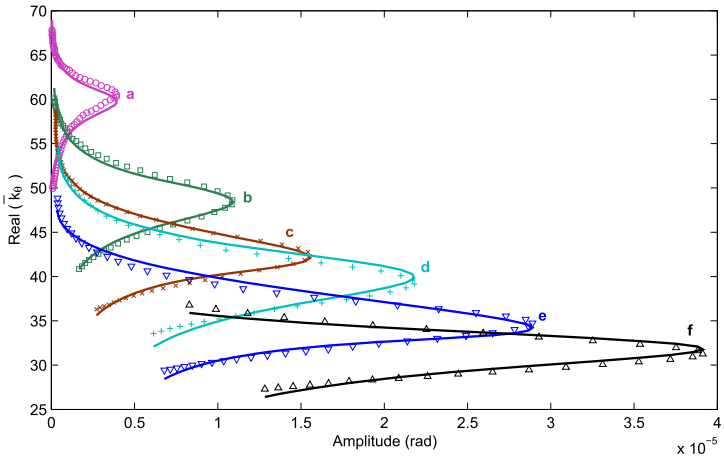

Figure 11- Real part of $\bar{k}_\theta$ at different excitation amplitudes, experiments (dots) and fitted (lines)

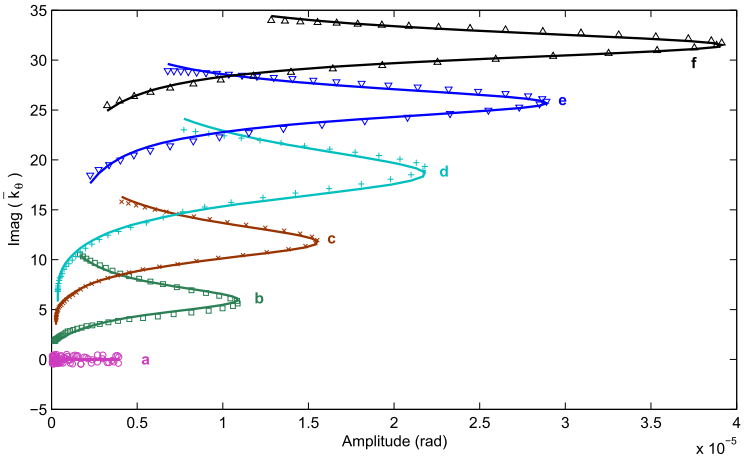

Figure 12- Imag. part of $\bar{k}_\theta$ at different excitation amplitudes, experiments (dots) and fitted (lines)

The abscissa in figures (10-12) are respectively the lateral and rotational movements of the beam at the frictional contact support- i.e point O- and is obtained by using the reference linear system, the identified equivalent linear models and the amplitude of the applied forces shown in figure (7).

Figure (10) shows that the identified values for $\bar{k}_w$ vary from -9.55 to -9.65. Since the sensitivity of the first mode with respect to $\bar{k}_w$ is low, it is reasonable to consider $\bar{k}_w$ to be constant in this range. Therefore from the results presented in figure (10) it can be concluded that the contact mechanism in

the normal direction is linear since a constant real value for $\bar{k}_w$ is obtained at all excitation amplitudes. The mean value of identified $\bar{k}_w$ is $\bar{k}_w = -9.6\times10^6 \ \ N/m$ which is considered as the constant value for the identified normal contact stiffness. As it was stated in previous section the normal contact stiffness obtained by using the natural frequencies, i.e. $k_w = 1\times10^7 \, N/m$, is not the optimum value for the first mode and needs to be modified. The negative value obtained for $\bar{k}_w$ in this section indicates that k_w must be decreased. Therefore the optimum value for normal contact stiffness is obtained as $k_n = 1\times10^7 - 9.6\times10^6 = 4\times10^5 \ \ N/m$. This shows that a linear stiffness model of the form $k_n w_o(t)$ governs the contact interface in normal direction; where $w_o(t)$ is the lateral movement of the contact point. It is worth mentioning that even though k_n is small and different from k_w , it can regenerate the natural frequencies with an acceptable accuracy. In Table 2 the first and second natural frequencies are compared for different values of k_w ,

Table 2- comparison of the first and second natural frequencies with experimental results

(@ $k_\theta = 152 \ \ Nm/rad$)

	First mode	*Second mode*
Experiment	*52.85*	*164.10*
$k_w = 1\times10^7 \ \ N/m$	*52.75*	*164.09*
Error (%)	*-0.18*	*0.0*
$k_n = 4\times10^5 \ N/m$	*51.78*	*153.5*
Error (%)	*-2.02*	*-6.45*

The contact stiffness in normal direction is calculated in above equal to $k_n = 4\times10^5 \ \ N/m$. The maximum displacement in normal direction based on figure 10 is about $X_{max} = 0.5\mu m$. Therefore the maximum normal contact force is approximately obtained as $N_{max} \approx k_n X_{max} = 0.2 \ \ N$. It is worth mentioning that the contribution of the damping mechanism in normal contact force is less than the stiffness mechanism. The maximum normal contact force is much less than the constant applied normal force *P*. Therefore the contact interface does not experience opening-closure and the macro-vibro-impact mechanism does not happen.

The results presented in figures (11) and (12) indicate that the contact mechanism in tangential direction is nonlinear since its equivalent linear model is a function of response amplitude and frequency. The equivalent stiffness, i.e $real(\bar{k}_\theta)$, decreases while the equivalent damping, i.e $imag(\bar{k}_\theta)$, increases as the response amplitude of the contact point is increased. It is found that the following stiffness and damping models govern the dynamics of the contact interface in tangential direction,

$$S(t) = \alpha_s \tanh\left(\beta_s \theta_o(t)\right) + \frac{\pi}{2}\gamma_s \left|\dot{\theta}_o(t)\right| sgn\left(\theta_o(t)\right) \tag{32}$$

$$D(t) = \left(\frac{\pi}{4}\alpha_d + \frac{\pi}{2}\beta_d \left|\theta_o(t)\right| + \gamma_d \left|\dot{\theta}_o(t)\right|\right) sgn\left(\dot{\theta}_o(t)\right) \tag{33}$$

$\theta_o(t)$ and $\dot{\theta}_o(t)$ in equations (32) and (33) are respectively the rotational movement and velocity of the contact point. In equation (32) the softening effect of the contact interfaces is approximated by using a tanh-type function [19]. Equation (33) is the friction model proposed by Anderson and Ferri [20]. By considering that the response is harmonic under harmonic excitation condition and employing the concept of describing functions [13], the following equivalent linear models are obtained for equations (32) and (33) [19],

$$S_e(X_\theta, \omega) = \frac{2\alpha_s}{\beta_s X_\theta}\left(-1 + \sqrt{(\beta_s X_\theta)^2 + 1}\right) + \gamma_s \omega \tag{34}$$

$$D_e(X_\theta, \omega) = j\left(\frac{\alpha_d}{X_\theta} + \beta_d + \gamma_d \omega\right) \tag{35}$$

where X_θ is the amplitude of $\theta_o(t)$. By fitting functions defined in equations (34) and (35) on the experimental results presented in figures (11) and (12) the model parameters are identified (Table (3)). The equivalent stiffness and damping models regenerated by identified parameters are compared with experimental results in figures (11) and (12). The results presented in figure (11) and (12) show that the nonlinear stiffness and damping models presented in equations (32) and (33) effectively model the dynamics of the contact interface in tangential direction.

Table 3-stiffness and damping model parameters at different load cases

Load case	α_s	β_s	γ_s	$\alpha_d \times 10^{-6}$	β_d	γ_d
a	*53.67*	*15.92*	*-2.43*	*0.0*	*0.0*	*0.0*
b	*92.96*	*15.95*	*-4.40*	*1.16*	*-766.85*	*2.37*
c	*91.8*	*15.97*	*-4.36*	*0.51*	*-959.83*	*2.98*
d	*102.21*	*15.97*	*-4.89*	*-3.14*	*-1253.5*	*3.90*
e	*96.60*	*14.45*	*-4.17*	*-6.64*	*-874.10*	*2.76*
f	*89.39*	*14.41*	*-3.86*	*-15.00*	*-675.88*	*2.17*

5. Conclusion

In this paper the dominant mechanisms in normal and tangential directions of a contact interface was characterized. Both nonlinear detection and parameter identification were considered. To this end, a method was proposed in this paper which can be used to detect the state- i.e. linear or nonlinear- of the behavior of multiple unknown elements in a nonlinear system. The input to the method is the measured nonlinear FRFs and the FRF matrix of a reference linear system. The proposed method was evaluated using numerical and experimental results.

6. References

[1] G.R. Tomlinson, Developments in the use of the Hilbert transform for detecting and quantifying nonlinearity associated with frequency response functions, Mech. Syst. Signal Pr. 1 (1997) 151–171.

[2] M. Mertens, I. Van Der Auweraer, P. Vanherck and R. Snoeys, The complex stiffness method to detect and identify nonlinear dynamic behavior of SDOF systems, Mech. Syst. Signal Pr. 3 (1989) 37-54.

[3] G. Kerschen, M. Peeters, A.F. Vakakis and J.C. Golinval, Nonlinear normal modes part 1: An attempt to demystify them, Mech. Syst. Signal Pr. 23 (2009) 170–194.

[4] M. Peeters, R. Viguie, G. Serandour, G. Kerschen and G.C. Golinval, Nonlinear normal modes part 2: Practical computation using numerical continuation techniques Mech. Syst. Signal Pr. 23 (2009) 195–216.

[5] Y.H. Chong and M. Imregun, Use of reciprocal vectors for nonlinearity detection, Arch. Appl. Mech. 70 (2000) 453–462.

[6] M. Feldman, Nonlinear system vibration analysis using the Hilbert transform—I. Free vibration analysis method 'FREEVIB', Mech. Syst. Signal Pr. 8 (1994) 119–127.

[7] A. Hot, G. Kerschen, E. Foltete, S. Cogan, Detection and quantification of non-linear structural behavior using principal component analysis, Mech. Syst. Signal Pr. 26 (2012) 104-116.

[8] M.B. Ozera, H.N. Ozguven, T.J. Royston, Identification of structural non-linearities using describing functions and the Sherman–Morrison method, Mech. Syst. Signal Pr. 23 (2009) 30–44.

[9] O. Arslan, M. Aykan, H.N. Ozguven, Parametric identification of structural nonlinearities from measured frequency response data, Mech. Syst. Signal Pr. 25 (2011) 1112–1125.

[10] E. Budak, H.N. Ozguven, 15th International Seminar on Modal Analysis A method for harmonic response of structures with symmetrical non-linearities, Leuven, Belgium 901–915, 1990.

[11] O. Tanrıkulu, B. Kuran, H.N. Ozguven, M. Imregun, Forced harmonic response analysis of non-linear structures, AIAA J. 31 (1993) 1313–1320.

[12] J. Sherman, W. J. Morrison, Adjustment of an inverse matrix corresponding to changes in the elements of a given column or a given row of the original matrix, Journal of Annals of Mathematical Statistics 20 (1949) 621–621.

[13] A. Gelb, W.E. Vander Velde. Multiple-input describing functions and nonlinear system design. McGraw-Hill Book Co., New York, 1968.

[14] H. Ahmadian, H. Jalali, F. Pourahmadian, Nonlinear model identification of a frictional contact support, Mech. Syst. Signal Pr. 24 (2010) 2844-2854.

[15] H. Jalali, H. Ahmadian, F. Pourahmadian, Identification of micro-vibro-impacts at boundary condition of a nonlinear beam, Mech. Syst. Signal Pr. 25 (2011) 1073–1085.

[16] G. Kerschen, J. C. Golinval, K. Worden, Theoretical and experimental identification of a nonlinear beam, Journal of Sound and Vibration 244 (2001) 597-613.

[17] K. Worden, G. R. Tomlinson, Nonlinearity in Structural Dynamics: Detection, Identification and Modeling, Institute of Physics Publishing, Bristol and Philadelphia, 2001.

[18] M.I. Friswell, J.E. Mottershead, Finite Element Model Updating in Structural Dynamics, Kluwer Academic Publishers, Dordrecht, 1995.

[19] S. Meyer, M. Link, Local non-linear softening behavior: modeling approach and updating of linear and nonlinear parameters using frequency response residuals, Proceedings of 21st International Modal Analysis Conference IMAC, 2003.

[20] J.R Anderson, A.A. Ferri, Behavior of a single-degree-of-freedom system with a generalized friction law, J.Sound Vib. 140 (1990) 287-304.

Highlight

A new approach for characterization of multiple unknown elements in nonlinear systems is developed. The method uses measured nonlinear FRFs and a reference linear system. The method is applied to numerical and experimental case studies.